MOLECULAR AND CELLULAR BIOLOGY, Nov. 1999, p. 7801–7815 Vol. 19, No. 11
0270-7306/99/$04.00+0

Saccharomyces cerevisiae pol30 (Proliferating Cell Nuclear Antigen) Mutations Impair Replication Fidelity and Mismatch Repair

CLARK CHEN,[1] BRADLEY J. MERRILL,[2,3] PATRICK J. LAU,[1] CONNIE HOLM,[2,3] AND RICHARD D. KOLODNER[1,3,4,5]*

Ludwig Institute for Cancer Research,[1] Department of Pharmacology,[2] Division of Cellular and Molecular Medicine,[3] Cancer Center,[4] and Department of Medicine,[5] University of California—San Diego School of Medicine, La Jolla, California 92093

Received 26 May 1999/Returned for modification 2 July 1999/Accepted 30 July 1999

To understand the role of *POL30* in mutation suppression, 11 *Saccharomyces cerevisiae pol30* mutator mutants were characterized. These mutants were grouped based on their mutagenic defects. Many *pol30* mutants harbor multiple mutagenic defects and were placed in more than one group. Group A mutations (*pol30-52*, *-104*, *-108*, and *-126*) caused defects in mismatch repair (MMR). These mutants exhibited mutation rates and spectra reminiscent of MMR-defective mutants and were defective in an in vivo MMR assay. The mutation rates of group A mutants were enhanced by a *msh2* or a *msh6* mutation, indicating that MMR deficiency is not the only mutagenic defect present. Group B mutants (*pol30-45*, *-103*, *-105*, *-126*, and *-114*) exhibited increased accumulation of either deletions alone or a combination of deletions and duplications (4 to 60 bp). All deletion and duplication breakpoints were flanked by 3 to 7 bp of imperfect direct repeats. Genetic analysis of one representative group B mutant, *pol30-126*, suggested polymerase slippage as the likely mutagenic mechanism. Group C mutants (*pol30-100*, *-103*, *-105*, *-108*, and *-114*) accumulated base substitutions and exhibited synergistic increases in mutation rate when combined with *msh6* mutations, suggesting increased DNA polymerase misincorporation as a mutagenic defect. The synthetic lethality between a group A mutant, *pol30-104*, and *rad52* was almost completely suppressed by the inactivation of *MSH2*. Moreover, *pol30-104* caused a hyperrecombination phenotype that was partially suppressed by a *msh2* mutation. These results suggest that *pol30-104* strains accumulate DNA breaks in a *MSH2*-dependent manner.

Cancer can be viewed as a genetic disease whereby the accumulation of mutations leads to the eventual activation of cellular oncogenes or inactivation of tumor suppressor genes (53). These events, in turn, confer growth or survival advantages to tumor cells. This framework predicts that genetic defects causing increased mutation rates should predispose cells to carcinogenesis. Such a prediction has been fulfilled by the discovery that inherited defects in DNA mismatch repair genes underlie the etiology of hereditary nonpolyposis colon carcinoma, a cancer predisposition syndrome (22, 44). Given this example, it seems likely that other genetic defects giving rise to mutator phenotypes should also contribute to carcinogenesis. One potential class of such mutator genes is the group of genes encoding DNA replication accessory factors, since these factors modulate the fidelity of DNA replication as well as participate in various aspects of DNA repair.

Proliferating cell nuclear antigen (PCNA) is a replication accessory factor encoded by the essential gene *POL30* in *Saccharomyces cerevisiae* (4). PCNA forms a homotrimeric ring around the DNA that serves as a binding platform for DNA polymerases. In doing so, PCNA enhances the processivity of DNA polymerases (26, 51). PCNA homologues from various eukaryotes share a high degree of sequence identity (19), and despite the lack of significant primary sequence homology between the *Escherichia coli* DNA polymerase III processivity factor and PCNA homologues, the three-dimensional crystal structures of these two proteins are superimposible (24, 26). This strong evolutionary conservation suggests that information obtained about PCNA in lower eukaryotes may be applicable to more complex organisms.

In addition to serving as a polymerase processivity factor, PCNA modulates the fidelity of DNA synthesis in vitro (41) as well as interacts with factors involved in nucleotide excision repair (9), mismatch repair (MMR) (18, 52), and base excision repair (42). PCNA also participates in the processing of branched DNA structures, including those formed during lagging-strand DNA synthesis (31, 56). The abundance of PCNA-interacting proteins led to the suggestion that PCNA may serve as a "docking bay" for many proteins and, in the process, coordinate various aspects of DNA synthesis and repair (19). Of the above-mentioned processes, DNA polymerase fidelity, MMR, and branch structure processing are mutation suppressing mechanisms pertinent to the results presented in this report.

Three major factors determine the ability of a polymerase to conduct faithful DNA replication, and all three are modulated by PCNA (5, 16, 30, 41): the selection of nucleotides that properly pair with the template (nucleotide discrimination), the 3′→5′ exonuclease activity that removes misincorporated nucleotides (proofreading), and adherence to the template during DNA replication (processivity). Defects in nucleotide discrimination or proofreading could lead to base substitution formation via nucleotide misincorporation. Failure of the DNA polymerase to adhere to the template properly could result in polymerase slippage, causing frameshifts, deletions, or duplications (27). Since specific types of mutations are associated with particular DNA polymerase defects, the defects of a

* Corresponding author. Mailing address: Ludwig Institute for Cancer Research, UCSD School of Medicine-CMME3080, 9500 Gilman Dr., La Jolla, CA 92093-0660. Phone: (619) 534-7804. Fax: (619) 534-7750. E-mail: rkolodner@ucsd.edu.

mutant polymerase may be inferred by an analysis of the types of mutations that it caused. For instance, the *pol2-4* allele in *S. cerevisiae* encodes a proofreading-deficient form of DNA polymerase ε that causes a roughly 10-fold increase in mutation rate. Not surprisingly, the mutation spectrum of *pol2-4* is notable for an increased accumulation of base substitutions (40). Another example is the *pol3-t* allele, which encodes a temperature-sensitive (ts) form of DNA polymerase δ. This mutation facilitates the formation of deletions flanked by short repeats, suggesting that *pol3-t* increases polymerase slippage (48, 49).

In addition to modulating polymerase fidelity, PCNA is also required for MMR in a human crude extract system (52). MMR is an evolutionarily conserved process which corrects misincorporated bases that escape DNA polymerase proofreading. Cells completely defective in MMR exhibit a 10- to 1,000-fold increase in the rate of mutation accumulation. Most of these mutations occur as frameshift mutations in mononucleotide runs (13, 35, 47). In *S. cerevisiae*, MMR initiates with the binding of mismatches by the MSH2-MSH6 or the MSH2-MSH3 heterodimer. Subsequent to this binding, other factors are recruited to the mismatch, leading to the eventual nicking, degradation, and resynthesis of the DNA strand containing the mutagenic nucleotide (23). In *E. coli*, this strand discrimination is mediated by (i) transient undermethylation of newly synthesized GATC sites by the Dam methylase and (ii) activation of MutH, the MMR-initiating endonuclease, to cleave the unmethylated DNA strand at hemimethylated GATC sites (38). The mechanism of strand discrimination in eukaryotes, where DNA methylation is probably not involved, is less clear. The observation that PCNA functions in MMR at a step prior to strand excision (14, 52) raises the possibility that PCNA functions at the initiation stages of MMR and that this may involve coupling of mismatch repair proteins to the replication machinery by PCNA (11, 22, 28, 39).

In vitro studies suggest that PCNA may participate in the processing of branched DNA structures via its interaction with RAD27 (31, 56). RAD27 (also known as RTH1, FEN1, MF-1, and exonuclease IV) is an evolutionarily conserved protein that has both a 5′ flap endonuclease and a 5′-to-3′ exonuclease activity. These activities are crucial for the processing of Okazaki fragments during DNA replication (32, 55). *S. cerevisiae rad27* mutants accumulate double-strand breaks (DSBs) and exhibit a strong mutator phenotype (47). The mutations that arise in *rad27* mutants are predominately duplications where the region duplicated is flanked by short stretches of imperfect direct repeats. These duplications are believed to result from mutagenic repair of DNA strand breaks involving misannealing of short single-stranded DNA tails (21, 47). Similar duplications have been reported as inactivating somatic mutations in the adenomatous polyposis coli as well as the p53 gene (12, 47).

Since PCNA participates in many processes that normally contribute to mutation suppression, we screened a panel of previously isolated *S. cerevisiae pol30* mutants for mutator phenotypes. Eleven *pol30* mutator mutants were identified. Mutation rate, spectrum, and epistasis analyses suggest that PCNA functions in multiple mutation-suppressing processes, ranging from polymerase fidelity to MMR. Detailed characterization of one MMR-defective mutant (*pol30-104*) yielded genetic evidence consistent with the notion that PCNA plays an important role in strand discrimination during MMR.

MATERIALS AND METHODS

General genetic methods. YPD (yeast extract-peptone-dextrose), sporulation, SD (synthetic dextrose), 5FOA (5-fluoroorotic acid), and canavanine media were prepared as previously described (6). Transformations were also performed as previously described (6). All strains were propagated at 37°C. Chromosomal DNA preparations were isolated by using glass bead lysis (18a) or Puregene kits (Gentra). PCR was performed in 50- to 100-μl reactions containing 0.5 U of Klentaq DNA polymerase (Ab Peptides), 0.08 U of *Pfu* DNA polymerase (Stratagene), 20 ng of genomic DNA, and 10 pmol of each primer in 1× PCII buffer (Ab Peptides). Primers were synthesized by the Dana-Farber Cancer Institute Molecular Biology Core Facility or Cybersyn Corp (Lenni, Pa.). Unless otherwise noted, standard three-temperature PCR was performed. Prior to DNA sequencing, PCR products were purified by using QIAquick Spin PCR purification kits (Qiagen). All DNA sequencing was performed with a Perkin Elmer/Applied Biosystems 377 DNA sequencer and dye terminator chemistry according to the manufacturer's instructions.

Mutation rates and recombination rates were calculated by fluctuation analysis using the method of the median in experiments with sets of five independent cultures as previously described (29, 35). For the recombination/chromosomal loss experiment, independent colonies of approximately 1.5-mm diameter were inoculated into 5 ml of YPD and grown overnight at 30°C. Appropriate dilutions were then plated onto SD complete as well as canavanine-containing plates. The colonies were scored after 3 days. The colonies on canavanine plates were then replica plated onto SD −Thr (threonine-deficient SD) plates, and the SD −Thr plates were scored after further incubation at 30°C for 1 day. Statistical comparisons were done by the Mann-Whitney test, the chi-square test statistic, or the two-tailed *t*-test statistics (7). All rates shown represent the average of two or more independent fluctuation analyses. Mutation spectra were determined by PCR amplification of target regions followed by DNA sequence analysis of one mutant per independent culture as previously described (6, 35, 47).

Overexpression of *RAD27* by pRDK762 in RDKY3578 was induced by inoculating isolates into SD −Ura containing 2% galactose and 2% raffinose. Appropriate dilutions of these cultures were grown to saturation at 30°C and then plated onto SD −Ura −Lys plates containing 2% galactose and 2% raffinose as well as SD −Ura plates containing 2% galactose and 2% raffinose. Colonies were scored after 5 days. Parallel experiments were performed with RDKY3588, which harbors the vector control. Mutation rates were calculated as described above.

Strain and plasmid construction. All haploid strains used were derivatives of S288C parental strains provided by Fred Winston (Harvard Medical School). Five series of strains, all derived from RDKY3023 (*MAT***a** *ura3-52 leu2Δ1 trp1Δ63 his3Δ200 lys2ΔBgl hom3-10 ade2Δ1 ade8*), were constructed. The first series (RDKY3546 to RDKY3548) was derived by transforming RDKY3023 with *TRP1* ARS-CEN plasmids bearing *pol30-41*, *-45*, and *-52* (pBL245-41, pBL230-45, pBL230-52; reagents kindly provided by Peter Burgers, Washington University, St. Louis, Mo. [3]). The *POL30* gene in the first series was disrupted with a *hisG-URA3-hisG* cassette by transforming with *Mlu*I-*Kpn*I-digested pBL243 (also provided by Peter Burgers) to generate the second series of strains, consisting of RDKY3549 to RDKY3551. Proper disruptions were verified by PCR amplification with 5′-TCA CAC TGA TGT AGT GGT GG and 5′-CCT GTT CCA CCG GCC CAG GG. The third series (RDKY3552 to RDKY3561) was derived by replacing *POL30* in RDKY3023 with *LEU2*-tagged *pol30* alleles by transformation with *Sac*I-digested pCH1572 (*POL30*), pCH1573 (*pol30-100*), pCH1575 (*pol30-102*), pCH1576 (*pol30-103*), pCH1577 (*pol30-104*), pCH1579 (*pol30-105*), pCH1580 (*pol30-106*), pCH1578 (*pol30-108*), pCH1637 (*pol30-126*), and pCH1638 (*pol30-114*) (2, 37). Proper integrants were confirmed by PCR amplification with 5′-CGA ATT GAC CTT CTA CTG GGA and 5′-TGT CGC CGA AGA AGT TAA GA. The fourth series (RDKY3543 and RDKY3562 to RDKY3569) was derived by disrupting the *MSH2* gene of the third series with a *hisG-URA3-hisG* cassette by transformation with *Aat*II-*Pvu*II-digested pRDK351 (35). Proper integrants were confirmed by PCR amplification with 5′-TCA AGT CAA TAC TTA AAC GCC and 5′-GAT TCG GTA ATC TCC GAA CAG AAG G. The fifth series (RDKY3544 and RDKY3570 to RDKY3577) was derived by disruption the *MSH6* gene of the third series with a *hisG-URA3-hisG* cassette by transformation with *Eco*RI-*Sph*I-digested pEAI108 (provided by Eric Alani, Cornell University). Proper integrants were confirmed by PCR amplification with 5′-CCA TTG ATG CGG ACG AAA ACT CGG and 5′-ATT TGC AAA GGG AAG GGA TG. RDKY3588 was constructed by transforming RDKY3560 with pCH1071 (*URA3 GAL*). RDKY3578 was constructed by transforming RDKY3560 with pRDK762 (*URA3 GAL-RAD27*). RDKY3668 was constructed by transforming RDKY3552 with pRDK762 (*URA3 GAL-RAD27*).

RDKY3545 was constructed by transforming RDKY3023 with pCH1511 (*URA3 POL30*). Likewise, RDKY3583 was constructed by transforming RDKY3556 with pCH1511 (*URA3 POL30*). 5′-GAA AAG ACG AAA AAT ATA GCG GCG GGC GGG TTA CGC GAC CGG TAT CGA GGC CTC CTC TAG TAC ACT C and 5′-TAA TAA ATA ATG ATG CAA ATT TTT TAT TTG TTT CGG CCA GGA AGC GTT GCG CGC CTC GTT CAG AAT G were used to amplify a *HIS3*-bearing *RAD52* disruptor fragment. This fragment was used to disrupt the *RAD52* gene in RDKY3583 to generate RDKY3585. The correct disruption was verified with 5′-ACG ACA CAT GGA GGA AAG AAA AAC T and 5′-CTC TCC CGT TAG TGA TTC TCG ATG. RDKY3584 was constructed by transforming RDKY2709, a strain that is isogenic to RDKY3023 except that the *MSH2* gene is disrupted with *hisG*, with pCH1511 (*URA3 POL30*). *POL30* in this strain was replaced with *pol30-104.LEU2* by transformation with *Sac*I-digested pCH1577 (2). Finally, the *RAD52* gene in this strain was disrupted as described above to generate RDKY3586. RDKY3587 and

RDKY3669 were constructed by transforming RDKY3586 and RDKY3585, respectively, with pRDK447 (*TRP1 MSH2*).

The diploid strain RDKY3579 was derived by crossing CH2165 (*MAT***a** *ura3-52 leu2 LEU2.POL30*) and CH2338 (*MAT*α *leu2 can1-51 hom3*). RDKY3581 was derived by crossing CH2161 (*MAT***a** *ura3-52 leu2 LEU2 pol30-104*) and CH2340 (*MAT*α *leu2 can1-51 hom3 LEU2.pol30-104*). 5′-ATG TCC TCC ACT AGG CCA GAG CTA AAA TTC TCT GAT GTA TCA GAG AGC AGC TGA AGC TTC GTA CGC and 5′-TTA TAA CAA CAA GGC TTT TAT ATA TTT CAG GTA ATT ATC GTT TTC CTT TTG CAT AGG CCA CTA GTG GAT CTG were used to PCR amplify a G418-bearing *MSH2* disruptor fragment (54). The *MSH2* gene in CH2165, CH2338, CH2161, and CH2340 was disrupted with the PCR fragment. Proper disruptions were confirmed by PCR amplification with 5′-CCA AAA ATC CAA TCA GAA CTC CAG and 5′-TGT ACC CAA TTC GTT CGG ACC TA. The resulting strains were crossed to yield RDKY3580 and RDKY3582. The genotypes of all diploids generated were further verified with *POL30*-specific primers (5′-CGA ATT GAC CTT CTA CTG GGA and 5′-TGT CGC CGA AGA AGT TAA GA) and *MSH2*-specific primers (5′-CCA AAA ATC CAA TCA GAA CTC CAG and 5′-TGT ACC CAA TTC GTT CGG ACC TA). All strains constructed for the purpose of this study are shown in Table 1.

A two-step method was used to construct the *GAL-RAD27* overexpression plasmid (pRKY762). In the first step, the *RAD27* gene was amplified from genomic DNA by using primers 5′-GAG CTC GAG ATG GGT ATT AAA GGT TTG AAT G and 5′-GCG CTC GAG CGA TGG TTC CGA TAT GCC AAA AGC. The resulting PCR fragment contains *Ava*I sites on both ends of *RAD27*. The fragment was gel purified, digested with *Ava*I and *Hin*dIII (cleaves at +1393 of *RAD27*), and ligated into *Sal*I-*Hin*dIII-digested YEp352 (*URA3* 2μm). The second step involved excising the *RAD27* coding region plus 12 bp of plasmid by digestion with *Bam*HI-*Hin*dIII and ligating this fragment into *Bam*HI-*Hin*dIII digested pCH1071 (pGAL YCp50). The resulting construct was sequenced with the following primers to verify that the *RAD27* fragment cloned was free of mutations: 5′-ATG GGT ATT AAA GGT TTG AAT G, 5′-TAC CGT TAT CAA TCA TTC TCA GTG, 5′-TCA AGA AGG GTG GAA ACA GAA A, 5′-GGC GAC CAT TTC AAG TTT ATT TC, 5′-TCG CCA CCA AAG GAG AAG GAA CT, and CGA TGG TTC CGA TAT GCC AAA AGC. pRKY762 was shown to fully rescue the ts, methyl methanesulfonate-sensitive (MMS^s), and mutator phenotypes of *rad27* null mutants in both glucose- and galactose-containing media.

In vivo MMR assay. The phagemids and most methods used to construct the mismatch-containing heteroduplexes were as previously reported (25). The heteroduplexes were purified by either benzoylated naphthoylated DEAE-cellulose chromatography followed by exonuclease V digestion (33) or high-pressure liquid chromatography (1). Comparable results were obtained in assays using substrates purified by using either protocol. The heteroduplex DNA was transformed into appropriate *S. cerevisiae* strains via lithium acetate or electroporation transformation. The transformants were plated onto SD −Ura plates supplemented with 6 mg of adenine per liter, incubated at 37°C, and scored after 5 days.

RESULTS

***POL30* mutants exhibit variable increases in spontaneous mutation rates.** We screened a panel of previously isolated *S. cerevisiae pol30* mutants (2, 3) for mutator phenotypes. Since many of the *pol30* mutants were cold sensitive, mutation rates were assessed at 37°C. Three mutator assays were used: an assay that scores for arginine permease inactivation (*CAN1*), an assay that detects reversion of a +4 insertion in the *LYS2* gene (*lys2-Bgl*), and an assay that detects reversion of a +1 insertion in the *HOM3* gene (*hom3-10*) (13, 35, 47). Whereas the *lys2-Bgl* and the *hom3-10* assays are particularly sensitive indicators of defective MMR, the *CAN1* assay is less specific for defective MMR and more sensitive to other mutagenic pathways (6, 13, 35, 47, 50). Eleven of the twelve mutants examined exhibited elevated mutation rates in all three assays (Table 2, set A). Of these mutants, *pol30-52* and *-104* exhibited the most dramatic mutator phenotypes, particularly in assays sensitive to defective MMR (41- and 21-fold increases in *lys2-Bgl*, respectively; 243- and 324-fold increases in *hom3-10*, respectively). However, these increases were lower (Mann-Whitney test, $P < 0.05$) than those caused by an *msh2* mutation, a mutation thought to completely inactivate MMR (82-fold in *lys2-Bgl*; 500-fold in *hom3-10*). These observations suggest that *pol30-52* and *-104* did not completely inactivate MMR. The comparable *CAN1* mutation rates of the *pol30-52*, *pol30-104*, and *msh2* mutants (15-, 26-, and 18-fold increases, respectively), then, suggests that *pol30-52* and *-104* caused mutagenic defects that are not related to MMR in addition to causing partial defects in MMR. The mutator phenotypes of the other *pol30* mutants were more subtle. *pol30-100*, *-108*, *-126*, and *-114* caused modest rate elevations that were most evident in the *hom3-10* assay. *pol30-41*, *-45*, *-102*, *-103*, and *-105* caused weak rate elevations in all three assays.

Since *pol30-52* exerts a dominant negative effect on cellular growth and sensitivity to DNA-damaging agents (3), we tested whether *pol30-52* exerts a dominant negative effect with regard to its mutator phenotype. Although the mutation rates in a *pol30-52*/*POL30* strain were lower than those of a *pol30-52* strain (Table 2, set a), these rates were still significantly elevated relative to those of a wild-type strain. This dominant negative effect was not due to the presence of an additional copy of *POL30* since a *POL30*/*POL30* strain exhibited mutation rates comparable to those of a wild-type strain. Similar partial dominant mutator effects were observed in *pol30-104*/*POL30* strains in patch assays (data not shown).

***POL30* mutants can be divided into distinct categories based on *CAN1* mutation spectra.** Although the assays used in this study are differentially sensitive to various mutagenic defects, they are not completely specific. Thus, it is difficult to determine the mutagenic defects of *pol30* mutants based solely on mutation rate analyses. Because the analysis of mutations accumulated in mutator mutants have been instrumental in deciphering the mechanism of mutagenesis (6, 8, 13, 35, 47, 48), we determined the mutation spectra of the various *pol30* mutants. The *CAN1* assay was selected for this purpose because it is sensitive to a variety of mutational events, including base substitutions, frameshifts, deletions, duplications, inversions, and translocations (6, 35, 47). Given the large number of *pol30* alleles studied and the absence of rationale for focusing on a specific allele, we sequenced 20 to 30 *CAN1*-inactivating mutations isolated from each *pol30* mutant (Tables 3 and 4).

To estimate the rate with which each type of mutations accumulated in the various *pol30* mutants (Table 5), we multiplied the proportion of each type of mutation (Table 3) by the *CAN1* mutation rate (Table 2, set a). Based on the rate of accumulating various types of mutations, the *pol30* mutants were divided into groups. Some mutants were placed in more than one group; this reflects the likelihood that some of the *pol30* mutations cause more than one defect due to the multifunctional nature of PCNA. Group A mutants (*pol30-52*, *-104*, *-108*, and *-126*) exhibited a greater tendency to accumulate frameshifts than base substitutions, an observation reminiscent of strains completely defective in MMR, such as *msh2* (35, 47). The rates of accumulating frameshift mutations in *msh2* and *pol30-52*, *-104*, *-108*, and *-126* strains were elevated 60-, 48-, 76-, 8-, and 6-fold, respectively, relative to wild-type strains, whereas the rates of accumulating base substitution mutations were elevated only 4-, 5-, 11-, 4-, and 4-fold, respectively (Table 5).

Group B mutants (*pol30-45*, *-103*, *-105*, *-126*, and *-114*) accumulated either deletions or a combination of deletions and duplications in addition to base substitutions and frameshifts. *pol30-103* and *-105* strains accumulated only deletions (36 to 60 bp), whereas *pol30-45*, *-126*, and *-114* accumulated both deletions (4 to 39 bp) and duplications (13 to 38 bp). The percentage of deletions and duplications was small in some *pol30* mutants. However, the detection of one deletion or duplication in a sample size of 30 translates to approximately 10^{-8} deletion/duplication events per cell per generation. This rate represents a significant increase over the rate of accumulating such mutations in wild-type cells, which is approximately 10^{-10}

TABLE 1. *S. cerevisiae* strains used in this study

Strain	Genotype
RDKY3023[a]	*MAT***a** *ura3-52 leu2Δ1 trp1Δ63 his3Δ200 lys2ΔBgl hom3-10 ade2Δ1 ade8*
RDKY2706	*MAT***a** *ura3-52 leu2Δ1 trp1Δ63 his3Δ200 lys2ΔBgl hom3-10 ade2Δ1 ade8 MSH2::hisG*
RDKY3545	*MAT***a** *ura3-52 leu2Δ1 trp1Δ63 his3Δ200 lys2ΔBgl hom3-10 ade2Δ1 ade8* [*URA3 POL30*]
RDKY3546	*MAT***a** *ura3-52 leu2Δ1 trp1Δ63 his3Δ200 lys2ΔBgl hom3-10 ade2Δ1 ade8* [*TRP1 pol30-41*]
RDKY3547	*MAT***a** *ura3-52 leu2Δ1 trp1Δ63 his3Δ200 lys2ΔBgl hom3-10 ade2Δ1 ade8* [*TRP1 pol30-45*]
RDKY3548	*MAT***a** *ura3-52 leu2Δ1 trp1Δ63 his3Δ200 lys2ΔBgl hom3-10 ade2Δ1 ade8* [*TRP1 pol30-52*]
RDKY3549	*MAT***a** *ura3-52 leu2Δ1 trp1Δ63 his3Δ200 lys2ΔBgl hom3-10 ade2Δ1 ade8 POL30::hisG-URA3-hisG* [*TRP1 pol30-41*]
RDKY3550	*MAT***a** *ura3-52 leu2Δ1 trp1Δ63 his3Δ200 lys2ΔBgl hom3-10 ade2Δ1 ade8 POL30::hisG-URA3-hisG*[*TRP1 pol30-45*]
RDKY3551	*MAT***a** *ura3-52 leu2Δ1 trp1Δ63 his3Δ200 lys2ΔBgl hom3-10 ade2Δ1 ade8 POL30::hisG-URA3-hisG*[*TRP1 pol30-52*]
RDKY3552	*MAT***a** *ura3-52 leu2Δ1 trp1Δ63 his3Δ200 lys2ΔBgl hom3-10 ade2Δ1 ade8 LEU2.POL30*
RDKY3553	*MAT***a** *ura3-52 leu2Δ1 trp1Δ63 his3Δ200 lys2ΔBgl hom3-10 ade2Δ1 ade8 LEU2.pol30-100*
RDKY3554	*MAT***a** *ura3-52 leu2Δ1 trp1Δ63 his3Δ200 lys2ΔBgl hom3-10 ade2Δ1 ade8 LEU2.pol30-102*
RDKY3555	*MAT***a** *ura3-52 leu2Δ1 trp1Δ63 his3Δ200 lys2ΔBgl hom3-10 ade2Δ1 ade8 LEU2.pol30-103*
RDKY3556	*MAT***a** *ura3-52 leu2Δ1 trp1Δ63 his3Δ200 lys2ΔBgl hom3-10 ade2Δ1 ade8 LEU2.pol30-104*
RDKY3557	*MAT***a** *ura3-52 leu2Δ1 trp1Δ63 his3Δ200 lys2ΔBgl hom3-10 ade2Δ1 ade8 LEU2.pol30-105*
RDKY3558	*MAT***a** *ura3-52 leu2Δ1 trp1Δ63 his3Δ200 lys2ΔBgl hom3-10 ade2Δ1 ade8 LEU2.pol30-106*
RDKY3559	*MAT***a** *ura3-52 leu2Δ1 trp1Δ63 his3Δ200 lys2ΔBgl hom3-10 ade2Δ1 ade8 LEU2.pol30-108*
RDKY3560[b]	*MAT***a** *ura3-52 leu2Δ1 trp1Δ63 his3Δ200 lys2ΔBgl hom3-10 ade2Δ1 ade8 LEU2.pol30-126*
RDKY3561	*MAT***a** *ura3-52 leu2Δ1 trp1Δ63 his3Δ200 lys2ΔBgl hom3-10 ade2Δ1 ade8 LEU2.pol30-114*
RDKY3543	*MAT***a** *ura3-52 leu2Δ1 trp1Δ63 his3Δ200 lys2ΔBgl hom3-10 ade2Δ1 ade8 LEU2.POL30 msh2::hisG-URA3-hisG*
RDKY3562	*MAT***a** *ura3-52 leu2Δ1 trp1Δ63 his3Δ200 lys2ΔBgl hom3-10 ade2Δ1 ade8 LEU2.pol30-100 msh2::hisG-URA3-hisG*
RDKY3563	*MAT***a** *ura3-52 leu2Δ1 trp1Δ63 his3Δ200 lys2ΔBgl hom3-10 ade2Δ1 ade8 LEU2.pol30-102 msh2::hisG-URA3-hisG*
RDKY3564	*MAT***a** *ura3-52 leu2Δ1 trp1Δ63 his3Δ200 lys2ΔBgl hom3-10 ade2Δ1 ade8 LEU2.pol30-103 msh2::hisG-URA3-hisG*
RDKY3565	*MAT***a** *ura3-52 leu2Δ1 trp1Δ63 his3Δ200 lys2ΔBgl hom3-10 ade2Δ1 ade8 LEU2.pol30-104 msh2::hisG-URA3-hisG*
RDKY3566	*MAT***a** *ura3-52 leu2Δ1 trp1Δ63 his3Δ200 lys2ΔBgl hom3-10 ade2Δ1 ade8 LEU2.pol30-105 msh2::hisG-URA3-hisG*
RDKY3567	*MAT***a** *ura3-52 leu2Δ1 trp1Δ63 his3Δ200 lys2ΔBgl hom3-10 ade2Δ1 ade8 LEU2.pol30-108 msh2::hisG-URA3-hisG*
RDKY3568[b]	*MAT***a** *ura3-52 leu2Δ1 trp1Δ63 his3Δ200 lys2ΔBgl hom3-10 ade2Δ1 ade8 LEU2.pol30-126 msh2::hisG-URA3-hisG*
RDKY3569	*MAT***a** *ura3-52 leu2Δ1 trp1Δ63 his3Δ200 lys2ΔBgl hom3-10 ade2Δ1 ade8 LEU2.pol30-114 msh2::hisG-URA3-hisG*
RDKY3544	*MAT***a** *ura3-52 leu2Δ1 trp1Δ63 his3Δ200 lys2ΔBgl hom3-10 ade2Δ1 ade8 LEU2.POL30 msh6::hisG-URA3-hisG*
RDKY3570	*MAT***a** *ura3-52 leu2Δ1 trp1Δ63 his3Δ200 lys2ΔBgl hom3-10 ade2Δ1 ade8 LEU2.pol30-100 msh6::hisG-URA3-hisG*
RDKY3571	*MAT***a** *ura3-52 leu2Δ1 trp1Δ63 his3Δ200 lys2ΔBgl hom3-10 ade2Δ1 ade8 LEU2.pol30-102 msh6::hisG-URA3-hisG*
RDKY3572	*MAT***a** *ura3-52 leu2Δ1 trp1Δ63 his3Δ200 lys2ΔBgl hom3-10 ade2Δ1 ade8 LEU2.pol30-103 msh6::hisG-URA3-hisG*
RDKY3573	*MAT***a** *ura3-52 leu2Δ1 trp1Δ63 his3Δ200 lys2ΔBgl hom3-10 ade2Δ1 ade8 LEU2.pol30-104 msh6::hisG-URA3-hisG*
RDKY3574	*MAT***a** *ura3-52 leu2Δ1 trp1Δ63 his3Δ200 lys2ΔBgl hom3-10 ade2Δ1 ade8 LEU2.pol30-105 msh6::hisG-URA3-hisG*
RDKY3575	*MAT***a** *ura3-52 leu2Δ1 trp1Δ63 his3Δ200 lys2ΔBgl hom3-10 ade2Δ1 ade8 LEU2.pol30-108 msh6::hisG-URA3-hisG*
RDKY3576[b]	*MAT***a** *ura3-52 leu2Δ1 trp1Δ63 his3Δ200 lys2ΔBgl hom3-10 ade2Δ1 ade8 LEU2.pol30-126 msh6::hisG-URA3-hisG*
RDKY3577	*MAT***a** *ura3-52 leu2Δ1 trp1Δ63 his3Δ200 lys2ΔBgl hom3-10 ade2Δ1 ade8 LEU2.pol30-114 msh6::hisG-URA3-hisG*
RDKY3578[b]	*MAT***a** *ura3-52 leu2Δ1 trp1Δ63 his3Δ200 lys2ΔBgl hom3-10 ade2Δ1 ade8 LEU2.pol30-126* [pRDK762 (*URA3 GAL-RAD27*)]
RDKY3588[b]	*MAT***a** *ura3-52 leu2Δ1 trp1Δ63 his3Δ200 lys2ΔBgl hom3-10 ade2Δ1 ade8 LEU2.pol30-126* [pCH1071 (*URA3 GAL*)]
RDKY3668	*MAT***a** *ura3-52 leu2Δ1 trp1Δ63 his3Δ200 lys2ΔBgl hom3-10 ade2Δ1 ade8 LEU2.POL30* [pRDK762 (*URA3 GAL-RAD27*)]
RDKY3579	*MAT***a** *ura3-52 leu2 LEU2.POL30* *MAT*α *leu2 can1-51 hom3*
RDKY3580	*MAT***a** *ura3-52 leu2 LEU2.POL30 MSH2::G418* *MAT*α *leu2 can1-51 hom3 MSH2::G418*
RDKY3581	*MAT***a** *ura3-52 leu2 LEU2 pol30-104* *MAT*α *leu2 can1-51 hom3 LEU2 pol30-104*
RDKY3582	*MAT***a** *ura3-52 leu2 LEU2 pol30-104 MSH2::G418* *MAT*α *leu2 can1-51 hom3 LEU2 pol30-104 MSH2::G418*
RDKY3583	*MAT***a** *ura3-52 leu2Δ1 trp1Δ63 his3Δ200 lys2ΔBgl hom3-10 ade2Δ1 ade8 LEU2.pol30-104* [pCH1511 (*URA3 POL30*)]
RDKY3584	*MAT***a** *ura3-52 leu2Δ1 trp1Δ63 his3Δ200 lys2ΔBgl hom3-10 ade2Δ1 ade8 LEU2.pol30-104 msh2::HisG* [pCH1511 (*URA3 POL30*)]
RDKY3585	*MAT***a** *ura3-52 leu2Δ1 trp1Δ63 his3Δ200 lys2ΔBgl hom3-10 ade2Δ1 ade8 LEU2.pol30-104 rad52::His3* [pCH1511 (*URA3 POL30*)]
RDKY3586	*MAT***a** *ura3-52 leu2Δ1 trp1Δ63 his3Δ200 lys2ΔBgl hom3-10 ade2Δ1 ade8 LEU2.pol30-104 rad52::His3 msh2::hisG* [pCH1511 (*URA3 POL30*)]
RDKY3587	*MAT***a** *ura3-52 leu2Δ1 trp1Δ63 his3Δ200 lys2ΔBgl hom3-10 ade2Δ1 ade8 LEU2.pol30-104 rad52::his3 msh2::hisG* [pCH1511(*URA3 POL30*)] [pRDK447 (*TRP1 MSH2*)]
RDKY3669	*MAT***a** *ura3-52 leu2Δ1 trp1Δ63 his3Δ200 lys2ΔBgl hom3-10 ade2Δ1 ade8 LEU2.pol30-104 msh2::hisG* [pCH1511 (*URA3 POL30*)] [pRDK447 (*TRP1 MSH2*)]

[a] The nature of the *ade8* mutation in RDKY3023 was previously undetermined. In the course of this study, we determined that the *ade8* mutation resulted from the deletion of a CT dinucleotide at positions 104 and 105 (where the A of the initiating methionine codon is nucleotide +1).

[b] *pol30-112* was originally described as a mutation that changed nucleotide 719 from an A to a G (2). However, on resequencing the original *pol30-112* plasmid, we found that the originally described mutation was present along with a second T→A change at nucleotide position 443, resulting in a V→D change at amino acid position 148. Thus, the original *pol30-112* allele was a double mutant. When this double mutation was transferred to the strains constructed here by gene replacement, only the N-terminal T→A change at nucleotide position 443 was inherited and was responsible for the phenotypes observed. Because this resulted in the creation of a new allele, we have named this allele *pol30-126* in accordance with the numbering used in reference 2.

TABLE 2. Mutation rate analysis

Genotype	RDKY no.	Group(s)	Mutation rate[a]		
			CAN1	*hom3-10*	*lys2-bgl*
Set a (*pol30* mutants)					
POL30	3552		3.6×10^{-7} (1)	1.0×10^{-8} (1)	1.7×10^{-8} (1)
POL30/POL30	3545		3.3×10^{-7} (1)	1.2×10^{-8} (1)	1.9×10^{-8} (1)
pol30-41/POL30	3546		6.5×10^{-7} (2)	n.d.	6.9×10^{-8} (3)
pol30-45/POL30	3547		2.2×10^{-7} (1)	n.d.	1.8×10^{-8} (1)
pol30-52/POL30	3548		11×10^{-7} (3)	57×10^{-8} (57)	63×10^{-8} (37)
pol30-41	3549		6.4×10^{-7} (2)	2.7×10^{-8} (3)	4.1×10^{-8} (2)
pol30-45	3550	B	4.8×10^{-7} (1)	1.5×10^{-8} (2)	3.4×10^{-8} (2)
pol30-52	3551	A	55×10^{-7} (15)	243×10^{-8} (243)	70×10^{-8} (41)
pol30-100	3553	C	16×10^{-7} (4)	16×10^{-8} (16)	8.4×10^{-8} (5)
pol30-102	3554		6.8×10^{-7} (2)	2.2×10^{-8} (2)	2.8×10^{-8} (2)
pol30-103	3555	B, C	13×10^{-7} (4)	2.8×10^{-8} (3)	6.6×10^{-8} (4)
pol30-104	3556	A	94×10^{-7} (26)	324×10^{-8} (324)	35×10^{-8} (21)
pol30-105	3557	B, C	6.8×10^{-7} (2)	1.5×10^{-8} (2)	3.3×10^{-8} (2)
pol30-106	3558		3.6×10^{-7} (1)	0.9×10^{-8} (1)	1.6×10^{-8} (1)
pol30-108	3559	A, C	19×10^{-7} (5)	15×10^{-8} (15)	6.4×10^{-8} (4)
pol30-126	3560	A, B	22×10^{-7} (6)	19×10^{-8} (19)	8.6×10^{-8} (5)
pol30-114	3561	B, C	7.7×10^{-7} (2)	6.0×10^{-8} (6)	3.8×10^{-8} (2)
msh2	3543		64×10^{-7} (18)	500×10^{-8} (500)	140×10^{-8} (82)
Set b (*pol30 msh2* double mutants)					
msh2	3543		97×10^{-7} (27)	800×10^{-8} (800)	144×10^{-8} (85)
msh2 pol30-100	3562	C	**153×10^{-7} (43)**	742×10^{-8} (742)	157×10^{-8} (92)
msh2 pol30-102	3563		75×10^{-7} (20)	860×10^{-8} (860)	134×10^{-8} (79)
msh2 pol30-103	3564	B, C	**200×10^{-7} (54)**	**$3{,}363 \times 10^{-8}$ (3,363)**	**663×10^{-8} (390)**
msh2 pol30-104	3565	A	**310×10^{-7} (84)**	**$1{,}700 \times 10^{-8}$ (1,700)**	**251×10^{-8} (148)**
msh2 pol30-105	3566	B, C	127×10^{-7} (34)	740×10^{-8} (740)	155×10^{-8} (91)
msh2 pol30-108	3567	A, C	**297×10^{-7} (80)**	**$1{,}567 \times 10^{-8}$ (1,567)**	**274×10^{-8} (161)**
msh2 pol30-126	3568	A, B	97×10^{-7} (27)	$1{,}077 \times 10^{-8}$ (877)	140×10^{-8} (82)
msh2 pol30-114	3569	B, C	98×10^{-7} (27)	985×10^{-8} (985)	129×10^{-8} (76)
Set c (*pol30 msh6* double mutants)					
msh6	3544		21×10^{-7} (6)	5.8×10^{-8} (6)	2.6×10^{-8} (2)
msh6 pol30-100	3570	C	**90×10^{-7} (25)**	**44×10^{-8} (44)**	**16×10^{-8} (9)**
msh6 pol30-102	3571		20×10^{-7} (6)	4.5×10^{-8} (5)	2.2×10^{-8} (1)
msh6 pol30-103	3572	B, C	**84×10^{-7} (23)**	**17×10^{-8} (17)**	**15×10^{-8} (9)**
msh6 pol30-104	3573	A	**252×10^{-7} (70)**	**879×10^{-8} (879)**	**122×10^{-8} (72)**
msh6 pol30-105	3574	B, C	**48×10^{-7} (13)**	3.8×10^{-8} (4)	2.8×10^{-8} (2)
msh6 pol30-108	3575	A, C	**131×10^{-7} (36)**	**56×10^{-8} (56)**	**27×10^{-8} (16)**
msh6 pol30-126	3576	A, B	**55×10^{-7} (15)**	**37×10^{-8} (37)**	**11×10^{-8} (6)**
msh6 pol30-114	3577	B, C	**36×10^{-7} (10)**	**32×10^{-8} (32)**	**9×10^{-8} (5)**
Set d (presence or absence of RAD27 overexpression)					
wt	3552		ND	ND	1.0×10^{-8} (1)
wt (*GAL-RAD27*)	3668		ND	ND	1.8×10^{-8} (2)
pol30-126	3588	A, B	ND	ND	6.5×10^{-8} (7)
pol30-126 (*GAL-RAD27*)	3578	A, B	ND	ND	5.6×10^{-8} (6)

[a] Average of two or more experiments. Numbers in parentheses indicate fold induction relative to the wild-type (wt) mean value. *pol30 msh2* or *pol30 msh6* double mutants that are significantly higher than those for corresponding *msh2*, *msh6*, or *pol30* single mutants (Mann-Whitney test, $P < 0.05$) are in boldface. ND, not determined.

per cell per generation (5a). The deletion breakpoints in *pol30* mutants were flanked by direct imperfect repeats (3 to 7 bp), similar to those observed in *rad27* and *pol3-t* mutants. The duplications in *pol30* mutants were also similar to those seen in *rad27* mutants in that the region duplicated was flanked by direct imperfect repeats (5 to 7 bp) and that the duplication always included one of the flanking repeats. However, the duplications in *pol30* mutants were, on average, smaller than those seen in *rad27* mutants (27 bp versus 39 bp; chi-square test, $P < 0.05$). This difference was mainly due to the absence of duplications of >50 bp in *pol30* mutants.

The two remaining *pol30* mutator mutants could not be easily classified based on their mutation spectra. *pol30-100* caused a moderate increase in the rate of accumulating base substitution mutations (sixfold) and a small increase in the rate of accumulating frameshift mutations (twofold). *pol30-102* caused roughly equal increases (twofold) in the rate of accumulating base substitution and frameshift mutations.

The *lys2-Bgl* reversion spectrum of *pol30-104* suggests a defect in DNA MMR. Since mutants that are completely defective in MMR (e.g., *msh2*, *mlh1*, and *pms1*) exhibit a characteristic *lys2-Bgl* reversion spectrum (8, 13, 35), we wished to determine whether such a spectrum could be seen in any of the group A mutants. *pol30-104* was selected as a representative allele for this purpose. As shown in Fig. 1, all of the *pol30-104* Lys^+ revertants resulted from −1 frameshifts; 65% of these frame-

TABLE 3. *CAN1* mutation spectra for various *pol30* mutants

Genotype	Type of event	Frequency (%)	Mutation[a]
pol30-41			
	Gross deletions	0/22 (0)	
	Gross insertions	0/22 (0)	
	Frameshifts	7/22 (32)	
		1/22	G1→G0
		1/22	G2→G3
		1/22	G3→G2
		1/22	C1→C0
		1/22	T4→T3
		1/22	T6→T7
		1/22	T2→T1
	Base substitution	15/22 (68)	
		1/22	G→T
		1/22	G→A
		1/22	G→C
		4/22	C→T
		4/22	C→G
		1/22	C→A
		1/22	T→G
		2/22	A→T
	Complex events	0/21 (0)	
pol30-45			
	Gross deletions	1/23 (4)	39 bp[1]
	Gross insertions	1/23 (4)	38 bp[2]
	Frameshifts	1/23 (4)	C1→C0
	Base substitution	20/23 (88)	
		1/23	C→T
		2/23	C→A
		3/23	C→G
		3/23	G→A
		4/23	G→C
		2/23	G→T
		1/23	T→A
		1/23	T→G
		1/23	T→C
		1/23	A→T
		1/23	A→G
	Complex events	0/23 (0)	
pol30-52			
	Gross deletions	0/20 (0)	
	Gross insertions	0/20 (0)	
	Frameshifts	16/20 (80)	
		2/20	G4→G3
		1/20	G0→G1
		1/20	A3→A2
		5/20	A6→A5
		1/20	A2→A3
		1/20	A6→A7
		1/20	T5→T4
		1/20	T3→T2
		1/20	T4→T3
		2/20	T6→T7
	Base substitution	4/20 (20)	
		1/20	C→T
		1/20	T→C
		1/20	A→T
		1/20	A→G
	Complex events	0/20 (0)	
pol30-100			
	Gross deletions	0/21 (0)	
	Gross insertions	0/21 (0)	
	Frameshifts	2/21 (10)	
		1/21	T6→T7
		1/21	G2→G1
	Base substitution	19/21 (90)	
		2/21	G→T
		3/21	G→A
		2/21	G→C

Continued on following page

TABLE 3—*Continued*

Genotype	Type of event	Frequency (%)	Mutation[a]
		1/21	C→T
		2/21	C→G
		4/21	C→A
		1/21	T→G
		1/21	T→A
		1/21	A→G
		1/21	A→C
	Complex events	0/21 (0)	
pol30-102			
	Gross deletions	0/29 (0)	
	Gross insertions	0/29 (0)	
	Frameshifts	9/29 (31)	
		3/29	T2→T1
		2/29	T1→T0
		1/29	T3→T4
		1/29	T6→T5
		2/29	C3→C2
	Base substitution	20/29 (69)	
		5/29	G→A
		3/29	G→T
		6/29	C→A
		3/29	C→T
		1/29	T→G
		1/29	T→C
		1/29	A→T
	Complex events	0/29 (0)	
pol30-103			
	Gross deletions	4/20 (20)	60 bp[3]
			40 bp[4]
			49 bp[5]
			41 bp[6]
	Gross insertions	0/20 (0)	
	Frameshifts	5/20 (25)	
		1/20	G3→G4
		1/20	A3→A4
		1/20	T6→T5
		2/20	T6→T7
	Base substitution	10/20 (50)	
		2/20	C→A
		5/20	G→T
		1/20	T→G
		2/20	C→G
	Complex events	1/20 (5)	
		1/20	TAT**g**GGTT**c**TTT-GG→TAT**t**GGTT**t**TTT**t**GG
pol30-104			
	Gross deletions	0/22 (0)	
	Gross insertions	0/22 (0)	
	Frameshifts	16/22 (73)	
		1/22	G1→G0
		1/22	G1→G2
		1/22	A6→A5
		1/22	C2→C1
		4/22	T4→T3
		7/22	T6→T7
		1/22	T1→T0
	Base substitution	6/22 (27)	
		2/22	G→T
		2/22	G→A
		1/22	C→G
		1/22	C→A
	Complex events	0/22 (0)	
pol30-105			
	Gross deletions	1/28 (4)	36 bp[7]
	Gross insertions	0/28 (0)	
	Frameshifts	5/28 (18)	
		3/28	T7→T6
		1/29	T6→T5
		2/28	T2→T1

Continued on following page

TABLE 3—*Continued*

Genotype	Type of event	Frequency (%)	Mutation[a]
		1/28	A2→A1
	Base substitution	21/28 (74)	
		4/28	G→A
		2/28	G→T
		6/28	C→A
		1/28	C→T
		1/29	C→G
		2/28	T→G
		2/28	T→C
		3/28	T→A
	Complex events	1/28 (4)	
pol30-108			
	Gross deletions	0/24 (0)	
	Gross insertions	0/24 (0)	
	Frameshifts	10/24 (42)	
		1/24	G3→G2
		1/24	G2→G1
		1/24	G1→G0
		1/24	A3→A2
		1/24	A5→A6
		1/24	T6→T5
		4/24	T6→T7
	Base substitution	14/24 (58)	
		3/24	G→T
		4/24	G→A
		1/24	G→C
		2/24	C→T
		4/24	C→A
	Complex events	0/24 (0)	
pol30-126			
	Gross deletions	2/22 (9)	4 bp[8]
			10 bp[9]
	Gross insertions	5/22 (23)	38 bp insertion[10]
			13 bp insertion[11]
			23 bp insertion[12]
			27 bp insertion[13]
			17 bp insertion[14]
	Frameshifts	5/22 (23)	
		2/22	G1→G0
		2/22	T7→T8
		1/22	C2→C1
	Base substitution	10/22 (45)	
		5/22	C→A
		1/22	G→A
		1/22	G→T
		2/22	C→G
		1/22	T→C
	Complex events	0/22 (0)	
pol30-114			
	Gross deletions	1/28 (4)	27 bp[15]
	Gross insertions	1/28 (4)	34 bp[16]
	Frameshifts	4/28 (14)	
		2/28	C2→C1
		1/28	C1→C0
		1/28	G1→G0
	Base substitution	19/28 (68)	
		1/28	C→T
		6/28	C→A
		3/28	C→G
		5/28	G→A
		3/28	G→C
		1/28	G→T
	Complex events	3/28 (10)	
		1/28	GTTTTcTCACAA→GTTTTtTtCACAA
		1/28	ATATcATATTTATttatGGG→ATATTTATTTATGCG
		1/28	AAGAGAGaGcTTGAG→AAGAGAGGTTGAG

[a] Superscript numbers correspond to those preceding the sequences in Table 4. Altered nucleotides are in lowercase; relevant microhomologies are in boldface.

TABLE 4. Sequences surrounding the junction of insertions and deletions

Genotype	Sequence[a]
pol30-45	[1]GTTGGT**TCC**...GTTGG**CTCC**TAAATTCCT
	[2]AATGGTGT**TAGCT***ttgctgccgcctatatctctattttcctgttct***tagct**TTGCTGCCGCCTATATCTCTATTTTCCTGTTCT**TAGCT**GTTTGGATC
pol30-103	[3]GGC**CGGCTT**...TCA**CGGCTT**TTGCACCAA
	[4]TTCTACAT**CATT**...CCATA**CAAT**CCTAAACTA
	[5]GGTGCTG**GGGTT**...GGTGCCT**GGGGT**CAAGGTATAATA
	[6]GGTGCTGG**GGTT**...AAACCCA**GGTG**CCTGGGGTC
pol30-105	[7]AGAC**ATC**T**A**...TATT**AAATA**CACTGGTG
pol30-126	[8]ATATCATA**TTTATTTAT**GGGTTCTTT
	[9]AAGTACAGT**AGTG**CGCTGA**AGTG**AAGAGAGA
	[10]CAATGGTG**TTAGC**T*tttgctgccgcctatatctctattttccctgttct**tag**C*TTTGCTGCCGCCTATATCTCTATTTTCCCTGTTC**TTAGC**TGTTTTG
	[11]TCACAGT**TTTCT***acaaaga**ttcct**t*ACAAAGA**TTCCT**TCCAGCATT
	[12]GTGTTAGC**TTTGCTG***ccgcctatatctctat**tttcctg***CCGCCTATATCTCTAT**TTTCCTG**TTCTTAGCT
	[13]TACCGG**CCCAGTTGG***attccgttattggagaaa**cccagtgg***ATTCCGTTATTGGAGAAA**CCCAGGTGG**CTGGGGTCC
	[14]ACGCTGAAGTG**AAGAGA***gagcttaagca**aagaga***GAGCTTAAGCA**AAGAC**ATATTGGTAT
pol30-114	[15]CA**TATTGGTA**C**TATTGGTA**CAGGTCTTTT
	[16]CTCT**ATGG**AAT^*attctgtca...a**atgg**ctac*ATTCTGTCA...**AATGG**CTAC

[a] Altered nucleotides are in lowercase; deleted sequences are underlined; inserted sequences are in italicized lowercase; ^ indicates that a space has been inserted. Relevant microhomologies are indicated in boldface.

shifts occurred in a run of 6 A's (nucleotides 664 to 669), 20% occurred in a run of four C's (nucleotides 697 to 700), and 10% occurred in a run of five T's (nucleotides 689 to 693). The distribution of these frameshift mutations is similar to those observed in *msh2*, *mlh1*, and *pms1* strains, further supporting the notion that *pol30-104* causes defective MMR.

An in vivo MMR assay indicates that *pol30-104*, *-108*, and *-126* cause defects in MMR. To directly assess the defects of group A mutants in MMR, various *pol30 ura3-52 ade2 ade8* strains were transformed with either an A/C or a G/T mismatch-containing *URA3 ADE8* plasmid (25). The mismatch resides in the *ADE8* gene such that only one strand of the plasmid encodes a functional protein. If the mismatch is corrected prior to DNA replication, the resulting colony will be nonsectored and either red or white. However, if the mismatch is not corrected, then the two *ADE8* alleles will segregate after replication, resulting in a red/white sectored colony. Thus, the efficiency of MMR in various *pol30* mutants can be assessed by scoring for Ura^+ sectored colonies. For comparison, we selected *pol30-103* from group B and *pol30-100*.

Comparable results were obtained using an A/C or a G/T substrate (Table 6). For the wild-type strain, 3% of all transformants were sectored. This percentage increased to approximately 60% in a MMR-defective strain (*msh2*). No significant percentage increase in sectored colonies was observed in *pol30-100* or *-103* mutants, indicating that these mutants are not defective in MMR. The group A mutants (*pol30-104*, *-108*, and *-126*) showed significant increases in the percentage of sectored colonies (to approximately 40, 25, and 14%, respectively), indicating that they are defective in MMR. Of these mutants, *pol30-104* mutants exhibited the largest increase in the sectoring phenotype. However, this increase is still significantly lower than that observed for a *msh2* mutant ($P < 0.005$), suggesting that *pol30-104*, *-108*, and *-126* all caused only partial defects in MMR. The same partial MMR defect was observed for *pol30-104* strains in two chromosome-based mutator assays (Table 2, set a). Overall, these results suggest that group A mutants are partially defective in MMR.

***lys2-Bgl* duplications in *pol30-126* mutants differ from those observed in *rad27* mutants.** The duplication mutations that arose in group B mutants were similar to those observed in *rad27* mutants (47). Since PCNA is known to stimulate the endo/exonucleolytic activity of RAD27 in vitro (31, 56), one interpretation of these observations is that group B mutants

TABLE 5. Summary of *CAN1* mutation spectra for *pol30* mutants[a]

Genotype	Group(s)	Substitution (%)	Frameshifts (%)	Deletions (%)	Insertions (%)	Complex events (%)
Wild type[b]		65 (1)	25 (1)	0	0	10
msh2[b]		15 (4)	85 (60)	0	0	0
pol30-41		68 (1)	32 (1)	0	0	0
pol30-45	B	88 (1)	4 (0.3)	4	4	0
pol30-52	A	20 (5)	80 (48)	0	0	0
pol30-100	C	90 (6)	10 (2)	0	0	0
pol30-102		69 (2)	31 (2)	0	0	0
pol30-103	B, C	50 (4)	25 (4)	20	0	0
pol30-104	A	27 (11)	73 (76)	0	0	0
pol30-105	B, C	74 (2)	18 (1)	4	0	4
pol30-108	A, C	58 (4)	42 (8)	0	0	0
pol30-126	A, B	45 (4)	23 (6)	9	23	0
pol30-114	B, C	68 (2)	14 (1)	4	4	10

[a] Indicated in parentheses is the fold increase in the estimated rate of frameshift and base substitution accumulation in various mutants over the wild-type rate. The estimated rates were calculated by multiplying the proportion of frameshifts and base substitutions (Table 2) by the respective *CAN1* mutation rates (Table 1). Group A mutants exhibit mutation rates and spectra reminiscent of mutants defective in MMR. Group B mutants accumulated either deletions or a combination of deletions and duplications in addition to base substitutions and frameshifts. Group C mutants exhibit mutation rates which were synergistic in the presence of a *msh6* mutation. Many *pol30* mutants harbor multiple mutagenic defects and were placed into more than one group.

[b] From reference 47.

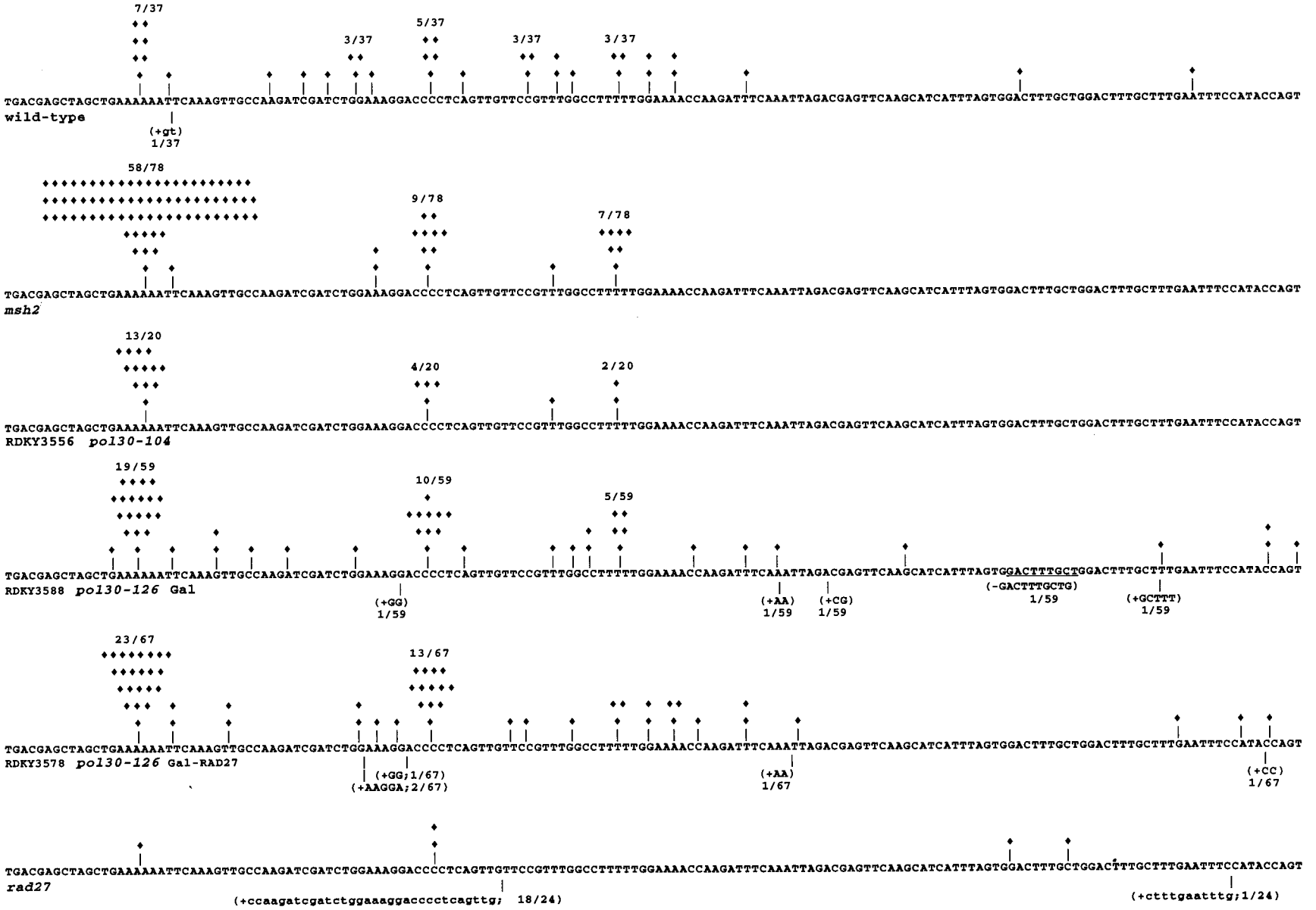

FIG. 1. *Lys2-Bgl* reversion spectra from wild-type, *msh2*, *rad27*, and *pol30* mutants. The sequence shown represents the reversion window (nucleotides 650 to 798) of the *lys2-Bgl* assay. The location of the nucleotide alteration resulting in functional restoration of *LYS2* is indicated by |. Each independent −1 frameshift is indicated by a ◆ above the deleted nucleotide. Duplications are indicated by (+) followed by the nucleotides inserted. Deletions of greater than one base pair are marked by (−) followed by the nucleotides deleted. The ratio indicated represents the proportion of each particular class of events. The wild-type and *msh2* spectra are from reference 8; the *rad27* spectra is from reference 47.

TABLE 6. In vivo MMR assay

Substrate	Genotype	RDKY no.	No. of sectored colonies[a]	Total no. of colonies[a]	% Sectoring[a]
A/C					
	Wild type	3023	57	1,783	3.2
	msh2	2706	843	1,400	60.2
	pol30-100	3553	116	2,723	4.3
	pol30-103	3555	71	2,192	3.2
	pol30-104	3556	439	1,025	42.8
	pol30-108	3559	83	293	28.3
	pol30-126	3560	401	2,513	15.9
G/T					
	Wild type	3023	85	3,142	2.7
	msh2	2706	943	1,455	64.8
	pol30-100	3553	99	2,255	4.4
	pol30-103	3555	66	1,801	3.7
	pol30-104	3556	238	704	33.8
	pol30-108	3559	249	1,140	21.8
	pol30-126	3560	183	1,701	10.7

[a] Results of a typical experiment, each repeated at least twice.

are defective in stimulating RAD27 activity. To explore this possibility, we tested whether galactose-induced RAD27 expression in a *pol30-126* strain would suppress duplication formation. *pol30-126* was selected because it exhibited the highest rate of duplication accumulation in group B. For this analysis we used the *lys2-Bgl* assay because the small mutation window in this system (0.5 kb versus 2.1 kb for *CAN1*) minimizes the sequencing effort necessary to obtain a large sample size (13, 35).

Galactose-induced RAD27 expression did not alter the *lys2-Bgl* reversion rate or spectrum of *pol30-126* mutants (Table 2, set d; Fig. 1). The RAD27-expressing plasmid was shown to fully rescue the ts, MMS^s, and mutator phenotypes of *rad27* null mutants in both glucose- and galactose-containing media (data not shown). When galactose induction was carried out in cells harboring the vector control plasmid or the RAD27 expression plasmid, approximately 90% of the Lys^+ revertants were −1 frameshifts; 10% were duplications or deletions, indicating that RAD27 function is not likely to be limiting in *pol30-126* mutants. Furthermore, the Lys^+ duplications that occurred in the *lys2-Bgl* assay in *pol30-126* mutants were different from those that occurred in *rad27* mutants. The *rad27 lys2-Bgl* revertants consisted of 21% −1 frameshifts and 79% duplications which involved duplication of unique segment of DNA bounded by short repeat sequences (47). In contrast, unlike the *pol30-126 CAN1* duplications (Table 3), the *pol30-126* Lys^+ duplications consisted of simple duplications of two or five nucleotides and did not involve duplication of a unique sequence bounded by repeated sequences. The *rad27* Lys^+ duplications were identical to the *rad27 CAN1* duplications, as both types of duplications involved duplication of unique sequences located between short imperfect repeats. Finally, the frameshift mutations in *pol30-126* mutants were different from those that occurred in *rad27* mutants. Approximately 50% of the −1 frameshifts in *pol30-126* were clustered at the same hot spots as those seen in mutants completely defective in MMR, such as *msh2*, *mlh1*, and *pms1* (8, 13, 35). This result is consistent with the partial defect that *pol30-126* mutants exhibited in the plasmid-based MMR assay. Such clustering was not observed for the *rad27* −1 frameshifts (47).

Epistasis analyses with *msh2* and *msh6* mutations suggest that *pol30* mutations also cause mutagenic defects that are distinct from defects in MMR. Except for group A mutants, the mutation spectra of *pol30* mutants differed from that of a *msh2* mutant, suggesting that *pol30* mutations cause defects in processes distinct from MMR. Additionally, mutation rate analyses of some group A mutants (*pol30-52* and *-104*) suggest that defective MMR constitutes only one of the mutagenic defects in these mutants. To explore these possibilities, we conducted an epistasis analysis between the various *pol30* mutations and a *msh2* mutation. In at least one mutator assay, double mutants containing a combination of *msh2* and *pol30-100*, *-103*, *-104*, or *-108* exhibited mutation rates significantly higher than that of a *msh2* or a *pol30* single mutant (Mann-Whitney test, $P < 0.05$) (Table 2, set b). This result indicates that *pol30-100*, *-103*, *-104*, and *-108* caused defects in processes distinct from MMR.

The disparity between the mutation rates of a *msh2* mutant and those of many *pol30* mutants makes the detection of synergistic effects difficult (Table 2, set b), especially if the *pol30* mutants are confined to accumulating base substitution mutations. We therefore compared the mutation rates of various *pol30 msh6* double mutants to those of *msh6* and *pol30* single mutants (Table 2, set c). Recall that MMR initiates with mismatch binding by either the MSH2-MSH6 heterodimer, which recognizes primarily base-base mispairs, or the MSH2-MSH3 heterodimer, which recognizes only insertion/deletion mispairs (10, 35). Since MSH2 is required for the formation of both complexes, *msh2* mutations completely inactivate MMR and cause a strong mutator phenotype. The mutation rates of *msh6* mutants are lower than those of *msh2* mutants but comparable to those of most *pol30* mutants. Because base-base mispairs are recognized by the MSH2-MSH6 heterodimer and not by the MSH2-MSH3 heterodimer (10, 35), *msh6* mutations completely inactivate MMR of base-base mispairs (23). Thus, the mutation rates in *msh6* strains primarily reflect increased accumulation of base substitution mutations. Of all of the mutations examined (Table 2, set c), *pol30-102* was the only one whose mutation rate was not enhanced by a *msh6* mutation. Of the remaining mutations, five (*pol30-100*, *-103*, *-105*, *-108*, and *-114*) exhibited synergistic mutator effects in the *CAN1* assay when combined with a *msh6* mutation. Because this synergy suggests that *pol30-100*, *-103*, *-105*, *-108*, and *-114* caused defects that increased polymerase misincorporation (see Discussion), these mutants were placed into group C. Many of the group C mutants also belonged to group A or B (Table 5).

A *msh2* mutation rescues the synthetic lethality between *pol30-104* and *rad52*. A series of genetic observations in *E. coli* raised an interesting hypothesis regarding the defect of group A mutants in MMR. The initial proposal of methyl-directed MMR in *E. coli* was based on the genetic observation that *dam* mutations were lethal in combination with *recA* mutations and that this lethality was suppressed by MMR-inactivating mutations, such as *mutS* (36). These observations were interpreted to mean that in the absence of a strand discriminating signal, the MMR machinery (e.g., MutH) aberrantly nicks both the parental and the daughter DNA strands, leading to DSBs which require RecA-mediated recombinational repair. When MMR is inactivated by a *mutS* mutation, DNA breaks are not generated, and RecA is no longer required for viability. The mechanism of daughter strand discrimination has yet to be described in eukaryotes. However, the recent observation that PCNA functions in MMR at a step prior to strand excision raises the possibility that it can facilitate strand discrimination (14, 52). If PCNA does facilitate strand discrimination in MMR, then defects leading to aberrantly initiated MMR may cause DNA breaks. Interestingly, a number of *pol30* mutations, including the group A mutations, were reported to be synthetically lethal with mutations in the *RAD52* series of genes—genes required for recombinational repair of DNA breaks

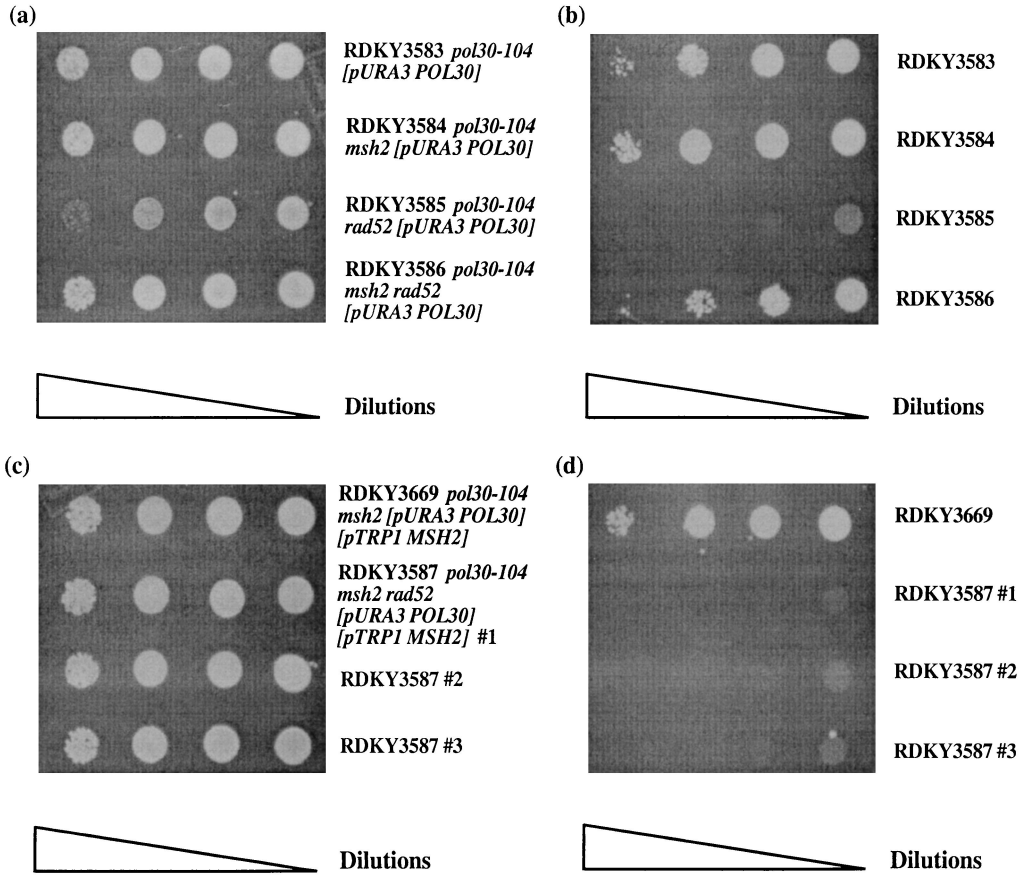

FIG. 2. A *msh2* mutation rescues the synthetic lethality between *pol30-104* and *rad52*. (a and b) *pol30-104* (RDKY3583), *pol30-104 msh2* (RDKY3584), *pol30-104 rad52* (RDKY3585) and *pol30-104 msh2 rad52* (RDKY3586) strains bearing a *URA3 POL30* plasmid were grown at 30°C in liquid SD −Ura to saturation; 10-fold serial dilutions of each culture were spotted onto an SD −Ura plate to determine viability (a) and an SD +5FOA plate to determine whether the *URA3 POL30* plasmid was required for viability (b). (c and d) *pol30-104 msh2* (RDKY3669) and three independent isolates of *pol30-104 msh2 rad52* (RDKY3587), all bearing *URA3 POL30* and *TRP1 MSH2* plasmids, were grown at 30°C in liquid SD −Ura −Trp media to saturation; 10-fold serial dilutions of each culture were spotted onto an SD −Ura −Trp plate to determine viability (c) and an SD −Trp +5FOA plate to determine whether the *URA3 POL30* plasmid was required for viability in the presence of the *TRP1 MSH2* plasmid (d).

(37). Thus, by analogy to the genetics of MMR in *E. coli*, a *msh2* mutation might rescue the synthetic lethality between *rad52* and group A mutations. Moreover, if the above analogy is appropriate, then *msh2* should not rescue the synthetic lethality between *rad52* and other *pol30* mutations.

To test these possibilities, the *RAD52* gene was disrupted in *pol30-104*, *pol30-100*, *pol30-103*, *pol30-104 msh2*, *pol30-100 msh2*, and *pol30-103 msh2* strains containing a Pol30$^+$ (*POL30 URA3*) plasmid. *pol30-104* was selected because it caused the strongest MMR defect among group A mutations. *pol30-100* and *-103* were selected because they exhibit synthetic lethality with *rad52* but do not cause MMR defects. The *pol30-104 rad52* [p*POL30 URA3*] strain did not grow on 5FOA plates, whereas the *pol30-104 msh2 rad52* [p*POL30 URA3*] strain grew, albeit with slightly reduced viability (Fig. 2a and b). These results indicate that the synthetic lethality between *pol30-104* and *rad52* was almost completely rescued by a *msh2* mutation. This suppression, as predicted, was abolished by the introduction of a *MSH2*-containing plasmid (Fig. 2c and d). The effect of the *msh2* mutation appeared specific for defects in *POL30* since *msh2* mutations did not suppress the MMS or the hydroxyurea sensitivity of *rad52* mutants (data not shown). *pol30-103 rad52*, *pol30-100 rad52*, *pol30-103 msh2 rad52*, and *pol30-100 msh2 rad52* strains containing a Pol30$^+$ plasmid were sensitive to killing by 5FOA (data not shown), suggesting that *MSH2* inactivation did not rescue the synthetic lethality between *pol30-100* or *pol30-103* and *rad52*. Similar to the behavior of *pol30-100* and *pol30-103*, a *RFC* allele exhibiting synthetic lethality with *rad52* that is not suppressed by *MSH2* inactivation has been reported (57). Together these studies suggest that the suppression of the synthetic lethality between *pol30-104* and *rad52* by *msh2* is allele specific.

A *msh2* mutation decreases the hyper-rec phenotype caused by *pol30-104*. Since DNA breaks are known to be recombinagenic (43) and since *pol30-104* strains accumulate DNA breaks (37), *pol30-104* might be expected to cause a hyperrecombination (hyper-rec) phenotype. Moreover, if the DNA strand breaks in *pol30-104* mutants occurred as a result of aberrantly initiated MMR, then the hyper-rec phenotype should be suppressed by a *msh2* mutation. To test this, we used a diploid strain carrying two recessive alleles (*can1-51* and *hom3*) on one copy of chromosome V; the other copy of chromosome V is wild type for both alleles (15, 17). Phenotypically, the strain is canavanine sensitive and prototrophic. However, if gene conversion at *CAN1* occurs or if there is a crossover between *CAN1* and the centromere followed by proper segregation, canavanine-resistant and homoserine prototrophic progeny will be obtained. On the other hand, loss of the wild-type

TABLE 7. Rates of heteroallelic recombination and chromosome loss in *msh2*, *pol30-104*, and *pol30-104 msh2* mutants

Strain	Rate[a]	
	Heteroallelic recombination	Chromosome loss
RKY3579 (wild type/wild type)	3.6×10^{-5} (1)	3.2×10^{-6} (1)
RKY3580 (*msh2*/*msh2*)	8.0×10^{-5} (2)	4.2×10^{-6} (1)
RKY3581 (*pol30-104*/*pol30-104*)	1.8×10^{-3} (50)	2.3×10^{-4} (72)
RKY3582 (*pol30-104 msh2*/*pol30-104 msh2*)	0.6×10^{-3} (17)	0.7×10^{-4} (22)

[a] Average of two more more experiments. Numbers in parentheses indicate fold induction relative to the wild-type rate. The Mann-Whitney test indicates that the recombination rate and the chromosomal loss rate in *pol30-104*/*pol30-104* mutants were significantly higher than those of *pol30-104 msh2*/*pol30-104 msh2* diploids ($P < 0.05$).

chromosome V will lead to canavanine-resistant but homoserine auxotrophic progeny.

As shown in Table 7, a *pol30-104* diploid strain had a 50-fold increase in mitotic recombination and a 72-fold increase in chromosome loss. A *msh2* mutation caused a twofold increase in mitotic recombination but had essentially no effect on chromosome loss. In the *pol30-104 msh2* double mutant, the rates of mitotic recombination and chromosome loss were higher than wild-type rates (17- and 22-fold, respectively). However, these rates were threefold lower ($P < 0.05$, Mann-Whitney) than those observed in *pol30-104* mutants. While the suppression of the *pol30-104* hyper-rec phenotype by *msh2* was modest in absolute terms, it was striking considering that *pol30-104* and *msh2* each independently caused a hyper-rec phenotype.

DISCUSSION

In this report, we described the effects of 12 *pol30* alleles on the rate of mutation accumulation. Eleven of the twelve *pol30* mutations studied caused increased accumulation of base substitutions, frameshifts, deletions, duplications, or some combination of these types of mutations. Although the *pol30* alleles studied here were previously shown to cause defects in DNA replication and to cause sensitivity to various DNA-damaging agents (2, 3, 37), we could not find any correlation between these phenotypes and the mutator phenotype of *pol30* mutants. The lack of such correlation suggests that the *pol30* mutants are simultaneously defective in multiple cellular processes. Consistent with this interpretation, many *pol30* mutations caused more than one mutagenic defect.

Based on their mutator phenotypes, the *pol30* mutants were divided into three groups. Because many *pol30* mutants harbor multiple mutagenic defects, they were placed in more than one group (Table 5). Group A mutations (*pol30-52*, *-104*, *-108*, and *-126*) caused MMR defects. Two of the group A mutations (*pol30-52* and *-104*) were previously reported to cause defects in MMR because they induce mutator phenotypes that were epistatic to MMR-inactivating mutations (18, 52). Our results extend these observations by demonstrating that *pol30-52* and *-104* strains exhibited mutation spectra indistinguishable from mutants completely inactivated for MMR, such as *msh2* (35, 47). Moreover, we showed that *pol30-104* strains are defective in the in vivo repair of plasmids containing mispaired bases. Using mutation spectra analysis and in vivo MMR defect as criteria, two additional MMR-defective *POL30* alleles, *pol30-108* and *-126*, were identified. *pol30-104* and *-108* were mutated at the same amino acid ($A_{251}V$ for *pol30-104* and $A_{251}T$ for *pol30-108*). Although these two alleles were similarly defective in terms of cold sensitivity and cell cycle arrest, *pol30-104* caused a significantly more severe MMS^s phenotype (2, 37) and a stronger mutator phenotype.

Although the mutator phenotypes of the *pol30-52* and *-104* strains were initially thought to result solely from defective MMR, two recent studies indicate that polymerase slippage also contributes to the *pol30-52* mutator phenotype (20, 57). Our mutation spectra analyses as well as the *msh2* and *msh6* epistasis analyses of *pol30-104*, *-108*, and *-126* suggest that these MMR-defective *pol30* alleles, like *pol30-52*, are additionally defective in some aspect of replicative fidelity. Contrary to the results presented here, Johnson et al. (18) reported that *pol30-104* caused a mutator phenotype that is epistatic to *msh2*, *mlh1*, and *pms1*. This discrepancy may be explained if the plasmid based dinucleotide instability assay used by Johnson et al. is more specific to MMR-related defects than our assays. The disagreement between our results and the reported epistatic relationship between *pol30-104* and *mlh1* in the *CAN1* assay (18) may have resulted from differences in strain background or from differences between a *mlh1* and a *msh2* mutation.

Group B mutants (*pol30-45*, *-103*, *-105*, *-126*, and *-114*) exhibited increased accumulation of either deletions alone or a combination of deletions and duplications. All of the *CAN1* duplications in *pol30* mutants, like those seen in *rad27* mutants, involved short repeated sequences at the breakpoint. Since PCNA stimulates the activity of RAD27 in vitro (31, 56), one interpretation of these observations is that group B mutants are defective in stimulating RAD27 activity. This interpretation suggests that group B mutants, like *rad27* mutants, accumulate DSBs and that these breaks are repaired by misannealing of single-stranded DNA tails (21, 47). However, two lines of evidence are inconsistent with this idea. First, the *lys2-Bgl* duplications in *pol30-126* mutants differed from those observed in *rad27* mutants. Second, the *CAN1* duplications in *pol30-126* mutants were, on average, shorter than those observed in *rad27* mutants. Finally, the duplications in *pol30-126* could not be suppressed by the expression of RAD27 under a *GAL10* promoter. Although the third observation could be explained by insufficient RAD27 expression, this explanation fails to account for the first two observations. One explanation that takes into account all three observations is that defective PCNA-DNA polymerase or PCNA-DNA interactions decreases the adherence of the polymerase to the template, thereby facilitating polymerase slippage. Consistent with this explanation, recent studies suggest that *pol30-52*, an allele defective in MMR, also induced replication slippage in the context of simple repeated sequences such as dinucleotide repeats (20, 57). Also, DNA polymerase mutants have been shown to accumulate repeat-mediated deletions and duplications (34, 48). While the above hypothesis is appealing, we cannot exclude the possibility that in the absence of wild-type PCNA, RAD27 may mediate the removal of some but not all of a flap structure. In vitro, however, RAD27 removes the entire flap structure in the absence of PCNA (32). We also cannot exclude that possibility

that the *pol30* mutants are defective in a yet to be identified repair system that specifically prevents deletion/duplication formation.

Group C mutants (*pol30-100*, *-103*, *-105*, *-108*, and *-114*) exhibited increased accumulation of base substitutions (Table 5) and synergistic mutator effects in the *CAN1* assay when combined with *msh6* mutations (Table 2, set c). The synergistic effect with *msh6*, a mutation thought to completely inactivate the repair of base-base mispairs, suggests that group C mutations increased polymerase misincorporation. Another interpretation of this synergy with *msh6* is that the *pol30* mutants are defective in *MSH3*-dependent MMR. This interpretation is unlikely because the mutator phenotype of *msh3 msh6* double mutants differed from those of group C *msh6* double mutants; *msh3 msh6* double mutants were potent mutators in the *hom3-10* and the *lys2-bgl* assay but were modest mutators in the *CAN1* assay (increases of roughly 500-, 100-, and 30-fold, respectively, over wild-type rates) (35). The group C *msh6* double mutants exhibited *CAN1* mutation rates comparable to that of *msh3 msh6* double mutants. However, the *hom3-10* and *lys2-bgl* reversion rates of group C *msh6* double mutants (ranging from increases of 6- to 15-fold over wild-type rates) were significantly lower than those of *msh3 msh6* double mutants.

Since the crystal structure of PCNA has been solved (26), we wished to determine whether group A, B, and C mutations were localized to any particular region of PCNA. The amino acids altered by group A mutations (*pol30-52*, *-104*, *-108*, and *-126*) were located in three distinct regions. *pol30-52* changed a residue located in the monomer-monomer interface region. *pol30-104*(*-108*) changed a residue in the beta sheets connecting the two monomer domains (i.e., the interdomain region). *pol30-126* changed a residue in one of the alpha helices contacting DNA. Therefore, we could not define a single region of PCNA where amino acid substitutions caused MMR defects. Likewise, group B and C mutations were not localized to any particular region of the PCNA structure. We were also unable to find any correlation between the known biochemical defects of *pol30* mutants and the severity of their defects in MMR. For instance, *pol30-52* trimers exhibited a notable decrease in stability relative to *pol30-104* trimers (7a). However, the two mutants were equally defective in MMR by the criteria established here.

Suppression of the *pol30-104 rad52* synthetic lethality and the *pol30-104*-induced hyper-rec phenotype by *MSH2* inactivation provides some insights into the mechanistic details of MMR. One interpretation of these results is that PCNA mediates a signal that targets newly synthesized DNA strands for excision during MMR. By analogy to the genetic interaction between mutations in *dam*, *recA*, and *mutS* in *E. coli* (36), in the absence of such a signal (as may be the case in a *pol30-104* mutant), the MMR machinery might nick both the template and the daughter DNA strands. Alternatively, in the absence of a strand discrimination signal, the MMR machinery can nick the template strand. In the presence of the many nascent strand breaks induced by *pol30-104* (37), these template strand nicks lead to the formation of DSBs. Another explanation is that PCNA couples MMR proteins to replication proteins. In this scenario, *pol30-104* causes replication fork stalling when MMR is initiated such that the stalled replication fork is converted to a DSB (46). These models are not mutually exclusive. We are currently testing these possibilities by isolating additional suppressors of the *pol30-104 rad52* synthetic lethality.

The observations reported here have a number of implications regarding the genetics of cancer susceptibility. First, the observation that many *pol30* mutants are mutators suggests that missense mutations in the human PCNA could increase cancer susceptibility. This possibility is particularly intriguing when one takes into consideration the partial dominant mutator effect of some *pol30* alleles, such as *pol30-52* and *-104*. Second, though many *pol30* mutants were by themselves weak mutators, their mutator effects were dramatically elevated in the presence of a *msh6* mutation. This observation suggests that weak *pol30* mutator alleles, which might exist as natural polymorphic variants in a population, could act as modifiers of partially defective MMR alleles, such as partial loss of function *MSH2* alleles or *MSH6* null alleles. Finally, *pol30*-induced duplications may lead to trinucleotide expansion, a process underlying the pathogenesis of many human neurological disorders (45). All of these possibilities await further examination.

ACKNOWLEDGMENTS

We thank John Weger and Pamela Hunt for DNA sequence analysis. We also thank Takuro Nakagawa, Abhijit Datta, Kyung Jae Myun, Alex Shoemaker, Richura Das Gupta, and Neelam Amin for helpful discussions and comments on the manuscript and Alex Shoemaker and Neelam Amin for resequencing the *pol30-126* allele.

This work was supported by NIH grants GM50006 to R.D.K. and GM36510 to C.H.

REFERENCES

1. **Alani, E., S. Lee, M. F. Kane, J. Griffith, and R. D. Kolodner.** 1997. *Saccharomyces cerevisiae MSH2*, a mispaired base recognition protein, also recognizes Holliday junctions in DNA. J. Mol. Biol. **265:**289–301.
2. **Amin, N. S., and C. H. Holm.** 1996. *In vivo* analysis reveals that the interdomain region of the yeast proliferating cell nuclear antigen is important for DNA replication and DNA repair. Genetics **144:**479–493.
3. **Ayyagari, R., K. J. Impellizzeri, B. L. Yoder, S. L. Gary, and P. M. J. Burgers.** 1995. A mutational analysis of the yeast proliferating cell nuclear antigen indicates distinct roles in DNA replication and DNA repair. Mol. Cell. Biol. **15:**4420–4429.
4. **Bauer, G. A., and P. M. Burgers.** 1990. Molecular cloning, structure and expression of the yeast proliferating cell nuclear antigen gene. Nucleic Acids Res. **18:**261–265.
5. **Bauer, G. A., and P. M. Burgers.** 1988. Protein-protein interactions of yeast DNA polymerase III with mammalian and yeast proliferating cell nuclear antigen (PCNA)/cyclin. Biochim. Biophy. Acta **951:**274–279.

5a. **Chen, C., and R. D. Kolodner.** Unpublished data.

6. **Chen, C., K. Umezu, and R. D. Kolodner.** 1998. Chromosomal rearrangements occur in *S. cerevisiae rfa1* mutator mutants due to mutagenic lesions processed by double-strand-break repair. Mol. Cell **2:**9–22.
7. **Daniel, W. W.** 1987. Biostatistics: a foundation for analysis in the health sciences, 5th ed. John Wiley & Sons, Inc., New York, N.Y.

7a. **Flores-Rozas, H.** Personal communication.

8. **Flores-Rozas, H., and R. D. Kolodner.** 1998. The *Saccharomyces cerevisiae MLH3* gene functions in *MSH3*-dependent suppression of frameshift mutations. Proc. Natl. Acad. Sci. USA **96:**12404–12409.
9. **Gary, R., D. L. Ludwig, H. L. Cornelius, M. A. MacInnes, and M. S. Park.** 1997. The DNA repair endonuclease XPG binds to proliferating cell nuclear antigen (PCNA) and shares sequence elements with the PCNA-binding regions of FEN-1 and cyclin-dependent kinase inhibitor p21. J. Biol. Chem. **272:**24522–24529.
10. **Genschel, J., S. J. Littman, J. T. Drummond, and P. Modrich.** 1998. Isolation of MutSbeta from human cells and comparison of the mismatch repair specificities of MutSbeta and MutSalpha. J. Biol. Chem. **273:**19895–19901.
11. **Gradia, S., D. Subramanian, T. Wilson, S. Acharya, A. Makhov, J. Griffith, and R. Fishel.** 1999. hMSH2-hMSH6 forms a hydrolysis-independent sliding clamp on mismatched DNA. Mol. Cell **3:**255–261.
12. **Greenblatt, M. S., A. P. Grollman, and C. C. Harris.** 1996. Deletions and insertions in the p53 tumor suppressor gene in human cancers: confirmation of the DNA polymerase slippage/misalignment model. Cancer Res. **56:**2130–2136.
13. **Greene, C. N., and S. Jinks-Robertson.** 1997. Frameshift intermediates in homopolymer runs are removed efficiently by yeast mismatch repair proteins. Mol. Cell. Biol. **17:**2844–2850.
14. **Gu, L., Y. Hong, S. McCulloch, H. Watanabe, and G. M. Li.** 1998. ATP-dependent interaction of human mismatch repair proteins and dual role of PCNA in mismatch repair. Nucleic Acids Res. **25:**1173–1178.
15. **Hartwell, L. H., and D. Smith.** 1985. Altered fidelity of mitotic chromosome transmission in cell cycle mutants of *S. cerevisiae*. Genetics **110:**381–395.
16. **Hindges, R., and U. Hubscher.** 1997. DNA polymerase delta, an essential enzyme for DNA transactions. Biol. Chem. **378:**345–362.
17. **Holm, C., T. Stearns, and D. Botstein.** 1989. DNA topoisomerase II must act

at mitosis to prevent nondisjunction and chromosome breakage. Mol. Cell. Biol. **9:**159–168.
18. **Johnson, R. E., G. K. Kovvali, S. N. Guzder, N. S. Amin, C. Holm, Y. Habraken, P. Sung, L. Prakash, and S. Prakash.** 1996. Evidence for involvement of yeast proliferating cell nuclear antigen in DNA mismatch repair. J. Biol. Chem. **271:**27987–27990.
18a. **Kaiser, C., S. Michaelis, and A. Mitchel.** 1994. A ten minute DNA prep from yeast. Methods Yeast Genet. **1994:**141–143.
19. **Kelman, Z., and J. Hurwitz.** 1998. Protein-PCNA interactions: a DNA-scanning mechanism. Trends Biochem. Sci. **1998:**236–238.
20. **Kokoska, R. J., L. Stefanovic, A. B. Buermeyer, R. M. Liskay, and T. D. Petes.** 1999. A mutation of the yeast gene encoding PCNA destabilizes both microsatellite and minisatellite DNA sequences. Genetics **151:**511–519.
21. **Kokoska, R. J., L. Stefanovic, H. T. Tran, M. A. Resnick, D. A. Gordenin, and T. D. Petes.** 1998. Destabilization of yeast micro- and minisatellite DNA sequences by mutations affecting a nuclease involved in Okazaki fragment processing (*rad27*) and DNA polymerase δ (*pol3-t*). Mol. Cell. Biol. **18:**2779–2788.
22. **Kolodner, R.** 1996. Biochemistry and genetics of eukaryotic mismatch repair. Genes Dev. **10:**1433–1442.
23. **Kolodner, R. D., and G. T. Marsischky.** 1999. Eukaryotic DNA mismatch repair. Curr. Opin. Genet. Dev. **9:**89–96.
24. **Kong, X. P., R. Onrust, M. O'Donnell, and J. Kuriyan.** 1992. Three-dimensional structure of the beta subunit of E. coli DNA polymerase III holoenzyme, a sliding DNA clamp. Cell **69:**425–437.
25. **Kramer, B., W. Kramer, M. S. Williamson, and S. Fogel.** 1989. Heteroduplex DNA correction in *Saccharomyces cerevisiae* is mismatch specific and requires functional *PMS* genes. Mol. Cell. Biol. **9:**4432–4440.
26. **Krishna, T. S. R., X. P. Kong, S. Gary, P. Burgers, and J. Kuriyan.** 1994. Crystal structure of the eukaryotic DNA polymerase processivity factor PCNA. Cell **79:**1233–1243.
27. **Kunkel, T. A.** 1992. DNA replication fidelity. J. Biol. Chem. **267:**18251–18254.
28. **Kunkel, T. A.** 1995. DNA-mismatch repair. The intricacies of eukaryotic spell-checking. Curr. Biol. **5:**1091–1094.
29. **Lea, D. E., and C. A. Coulson.** 1948. The distribution of the numbers of mutants in bacterial populations. J. Genet. **49:**264–285.
30. **Lee, S. H.** 1993. The 3′-5′ exonuclease of human DNA polymerase delta (pol delta) is regulated by pol delta accessory factors and deoxyribonucleoside triphosphates. Nucleic Acids Res. **21:**1935–1939.
31. **Li, X., J. Li, J. Harrington, M. R. Lieber, and P. M. Burgers.** 1995. Lagging strand DNA synthesis at the eukaryotic replication fork involves binding and stimulation of FEN-1 by proliferating cell nuclear antigen. J. Biol. Chem. **270:**22109–22112.
32. **Lieber, M. R.** 1997. The FEN-1 family of structure-specific nucleases in eukaryotic DNA replication, recombination, and repair. Bioessays **19:**233–240.
33. **Lin, Y. L., M. K. Shivji, C. Chen, R. Kolodner, R. D. Wood, and A. Dutta.** 1998. The evolutionarily conserved zinc finger motif in the largest subunit of human replication protein A is required for DNA replication and mismatch repair but not nucleotide excision repair. J. Biol. Chem. **273:**1453–1461.
34. **Liu, V., D. Bhaumik, and T. S.-F. Wang.** 1999. Mutator phenotype induced by aberrant replication. Mol. Cell. Biol. **19:**1126–1135.
35. **Marsischky, G. T., N. Filosi, M. F. Kane, and R. Kolodner.** 1996. Redundancy of *Saccharomyces cerevisiae* MSH3 and MSH6 in MSH2-dependent mismatch repair. Genes Dev. **10:**407–420.
36. **McGraw, B. R., and M. G. Marinus.** 1980. Isolation and characterization of Dam+ revertants and suppressor mutations that modify secondary phenotypes of dam-3 strains of *Escherichia coli* K-12. Mol. Gen. Genet. **178:**309–315.
37. **Merrill, B. J., and C. Holm.** 1998. The *RAD52* recombinational repair pathway is essential in *pol30* (PCNA) mutants that accumulate small single-stranded DNA fragments during DNA synthesis. Genetics **148:**611–624.
38. **Modrich, P.** 1987. DNA mismatch correction. Annu. Rev. Biochem. **56:**435–466.
39. **Modrich, P., and R. Lahue.** 1996. Mismatch repair in replication fidelity, genetic recombination, and cancer biology. Annu. Rev. Biochem. **65:**101–133.
40. **Morrison, A., and A. Sugino.** 1994. The 3′→5′ exonucleases of both DNA polymerase delta and epsilon participate in correcting errors of DNA replication in *Saccharomyces cerevisiae*. Mol. Gen. Genet. **242:**289–296.
41. **Mozzherin, D. J., M. McConnell, M. V. Jasko, A. A. Krayevsky, C. K. Tan, K. M. Downey, and P. A. Fisher.** 1996. Proliferating cell nuclear antigen promotes misincorporation catalyzed by calf thymus DNA polymerase delta. J. Biol. Chem. **271:**31711–31717.
42. **Muller-Weeks, S. J., and S. Caradonna.** 1996. Specific association of cyclin-like uracil-DNA glycosylase with the proliferating cell nuclear antigen. Exp. Cell Res. **226:**346–355.
43. **Osman, F., and S. Subramani.** 1998. Double-strand break-induced recombination in eukaryotes. Prog. Nucleic Acid Res. Mol. Biol. **58:**263–299.
44. **Peltomaki, P., and H. F. A. Vasen.** 1997. Mutations predisposing to hereditary nonpolyposis colorectal cancer: database and results of a collaborative study. Gastroenterology **113:**1146–1158.
45. **Ross, C. A., R. L. Margolis, M. W. Becher, J. D. Wood, S. Engelender, J. K. Cooper, and A. H. Sharp.** 1998. Pathogenesis of neurodegenerative diseases associated with expanded glutamine repeats: new answers, new questions. Prog. Brain Res. **117:**397–419.
46. **Seigneur, M., V. Bidnenko, S. D. Ehrlich, and B. Michel.** 1998. RuvAB acts at arrested replication forks. Cell **95:**419–430.
47. **Tishkoff, D. X., N. Filosi, G. M. Gaida, and R. D. Kolodner.** 1997. A novel mutation avoidance mechanism dependent on *S. cerevisiae RAD27* is distinct from DNA mismatch repair. Cell **88:**253–263.
48. **Tran, H. T., N. P. Degtyareva, N. N. Koloteva, A. Sugino, H. Masumoto, D. A. Gordenin, and M. A. Resnick.** 1995. Replication slippage between distant short repeats in *Saccharomyces cerevisiae* depends on the direction of replication and the *RAD50* and *RAD52* genes. Mol. Cell. Biol. **15:**5607–5617.
49. **Tran, H. T., D. A. Gordenin, and M. A. Resnick.** 1996. The prevention of repeat-associated deletions in *Saccharomyces cerevisiae* by mismatch repair depends on size and origin of deletions. Genetics **143:**1579–1587.
50. **Tran, H. T., J. D. Keen, M. Kricker, M. A. Resnick, and D. A. Gordenin.** 1997. Hypermutability of homonucleotide runs in mismatch repair and DNA polymerase proofreading yeast mutants. Mol. Cell. Biol. **17:**2859–2865.
51. **Tsurimoto, T.** 1998. PCNA, a multifunctional ring on DNA. Biochim. Biophys. Acta **1443:**23–39.
52. **Umar, A., A. B. Buermeyer, J. A. Simon, D. C. Thomas, A. B. Clark, R. M. Liskay, and T. A. Kunkel.** 1996. Requirement for PCNA in DNA mismatch repair at a step preceding DNA resynthesis. Cell **87:**65–73.
53. **Vogelstein, B., and K. W. Kinzler.** 1993. The multistep nature of cancer. Trends Genet. **9:**138–141.
54. **Wach, A., A. Brachat, R. Pohlmann, and P. Philippsen.** 1994. New heterologous modules for classical or PCR-based gene disruptions in *Saccharomyces cerevisiae*. Yeast **10:**1793–1808.
55. **Waga, S., and B. Stillman.** 1994. Anatomy of a DNA replication fork revealed by reconstitution of SV40 DNA replication in vitro. Nature **369:**207–212.
56. **Wu, X., J. Li, X. Li, C. L. Hsieh, P. M. Burgers, and M. R. Lieber.** 1996. Processing of branched DNA intermediates by a complex of human FEN-1 and PCNA. Nucleic Acids Res. **24:**2036–2043.
57. **Xie, Y., C. Counter, and E. Alani.** 1999. Characterization of the repeat-tract instability and mutator phenotypes conferred by a *Tn3* insertion in *RFC1*, the large subunit of the yeast clamp loader. Genetics **151:**499–509.